there is a real excess of low-redshift quasars in that region.

Further study of this excess will require a variety of new data. A complete sample of radio quasars covering the relevant areas, with complete identifications and confirmed redshifts, would help to dispel any lingering doubts regarding selection effects. Deep ultraviolet-excess or objective-prism quasar surveys in the 10–15 h zone, in conjunction with others made under identical conditions in other areas of the sky, would show any differences in redshift distribution at a high level of significance. [Unfortunately there are very few optically selected (non-radio) quasars in the 10–15 h zone; the two studies[11,12] in which more than a few quasars have been confirmed were both based on objective-prism data and geared specifically towards high-redshift (emission-line) objects, and are not useful in examining any possible excess of low-redshift quasars.] Source counts from deep radio and X-ray surveys would also help in studying differences between the populations in this direction and others. The X-ray background may also provide a constraint, although its origin is still a matter of debate; a weak (0.5%) dipole appears to be present, again coincident with the direction of motion towards the microwave background[13].

The structure implied by the distribution of low-redshift quasars may be complex—there is some indication of a relative deficiency in the direction of the south galactic pole—but it appears to be dominated by the excess in the 10–15 h zone. This feature has an overdensity of ~1–2, angular diameter ~30°–40°, and mean redshift ~0.3–0.4, although it is difficult to determine these parameters with any precision. At the corresponding distance of ~800 h^{-1} Mpc it would have a diameter of ~400 h^{-1} Mpc.

It may be significant that this large feature lies in the direction of our motion towards the microwave background (Fig. 1). It has recently been suggested[6–8] that distant galaxies out to ≥6,000 km s^{-1} share this motion. If indeed there is a bulk streaming motion in a region over 100 h^{-1} Mpc diameter surrounding us, the obvious interpretation is that it is due to the attraction of a very large mass lying beyond, in the direction of motion[14]. While asymmetries in the streaming motion suggest that the mass may not be too far beyond[7,8], the far more distant structure implied by the excess of low-redshift quasars (assuming they follow the mass) would also suffice to produce the 600 km s^{-1} streaming motion. From linear perturbation theory[15], this velocity can be produced with the parameters (overdensity, angular size and redshift) given above and a value for the cosmological density parameter Ω of the order of unity. Such an association between a distant mass and local kinematics would provide new information on large-scale properties of the universe.

I thank Ann Savage, Bob Sanders, Jasper Wall, and many other colleagues for helpful discussions. I am grateful for the hospitality of the CSIRO Division of Radiophysics and the Raman Research Institute, where part of this work was carried out.

Received 18 December 1986; accepted 24 February 1987.

1. Oort, J. H. *A. Rev. Astr. Astrophys.* **21**, 373–428 (1983).
2. Shaver, P. A. *Astr. Astrophys.* **136**, L9–L10 (1984).
3. Shanks, T., Fong, R., Boyle, B. J. & Peterson, B. A. in *Quasars* (eds Swarup, G. & Kapahi, V. K.) 37–43 (Reidel, Dordrecht, 1986).
4. Véron-Cetty, M.-P. & Véron, P. ESO Scientific Report No. 4 (1985).
5. Yahil, A., Walker, D. & Rowan-Robinson, M. *Astrophys. J.* **301**, L1–L5 (1986).
6. Collins, C. A., Joseph, R. D. & Robertson, N. A. *Nature* **320**, 506–508 (1986).
7. Burstein, D. *et al.* in *Galaxy Distances and Deviations from Universal Expansion* (eds Madore, B. F. & Tully, R. B.) 123–130 (Reidel, Dordrecht, 1986).
8. Dressler, A. *et al. Astrophys. J.* **313**, L37–L42 (1987).
9. Bolton, J. G., Savage, A. & Wright, A. E. *Aust. J. Phys. Astrophys. Suppl.* **46**, 1–27 (1979).
10. Large, M. I., Mills, B. Y., Little, A. G., Crawford, D. F. & Sutton, J. M. *Mon. Not. R. astr. Soc.* **194**, 693–704 (1981).
11. Osmer, P. S. & Smith, M. G. *Astrophys. J.* **213**, 607–618 (1977).
12. Kunth, D., Sargent, W. L. W. & Kowal, C. *Astr. Astrophys. Suppl.* **44**, 229–239 (1981).
13. Shafer, R. A. & Fabian, A. C. in *Early Evolution of the Universe and its Present Structure* (eds Abell, G. O. & Chincarini, G.) 333–343 (Reidel, Dordrecht, 1983).
14. Lynden-Bell, D. *Q. Jl R. astr. Soc.* **27**, 319–327 (1986).
15. Davis, M. & Peebles, P. J. E. *A. Rev. Astr. Astrophys.* **21**, 109–130 (1983).

Magnetospheric charge-exchange effect on the electroglow of Uranus

W. H. Ip

Max-Planck-Institut für Aeronomie, D-3411 Katlenburg-Lindau, FRG

One common feature of the magnetospheric systems of the outer planets explored by the Pioneer 10 and 11 and the Voyager 1 and 2 spacecraft is that extended distributions of neutral gas of planetary exospheric origin and/or of satellites–rings origin coexist with the magnetospheric plasma. This property invariably leads to the occurrence of charge-exchange loss of the charged particles in the inner magnetospheres of Jupiter, Saturn and Uranus. With emphasis on the Uranian system I examine here the idea that the injection of the recombined fast neutrals into the planetary upper atmosphere might be contributing in part to the generation of the dayside electroglow. The recent results from the Voyager 2 encounter also permit the idea that the associated impact ionization effect could be important in maintaining the nightside ionosphere.

The Voyager 2 encounter with Uranus[1] has produced a wealth of new information on this gaseous outer planet, its satellite and ring systems and a new type of magnetosphere. Because of the unique pointing direction of Uranus and the large tilt angle ($\theta \sim 60°$) between the dipole moment and the rotational axis[2], the general pattern of magnetospheric convection is now believed to be similar to that of the terrestrial magnetosphere but with the whole system in co-rotation with the planet[3–6]. In other words, unlike the cases with the jovian and saturnian magnetospheres[7,8], the sunward convection effect driven by a dawn-to-dusk electric field can penetrate very deep into the magnetosphere.

At the same time, according to the plasma science experiment[3] and the planetary radioastronomy experiment[9], there might be indications for the formation of a plasmapause separating the sunward-convecting plasma from the 'co-rotating' plasmasphere. Thus the streamlines (or equipotential lines) do not necessarily follow a rectilinear pattern with some of them directly intercepting the planet on the nightside hemisphere—as expected in the idealized situation with the tilt angle, $\theta \sim 90°$. The presence of a plasmapause structure at Uranus, however, is a complicated issue still to be investigated in detail.

Another result of major importance to atmospheric and magnetospheric physics has to do with the ultraviolet spectroscopy (UVS) observations of the so-called electroglow from the dayside hemisphere of Uranus[10,11]. The intense ultraviolet emissions from the H_2 and H I Rydberg series were found to be uniformly distributed over the dayside disk and the H Lyman-α emission brightness of 1.5 KR near the subsolar point is consistent with the International Ultraviolet Explorer (IUE) time-averaged value of 1.4 KR[12]. The characteristic property of non-solar excitation of the extreme ultraviolet (EUV) emissions (as found at Jupiter and Saturn) is also established in the case of Uranus[11]. One interesting difference, however, is that the H_2 emission spectra of Jupiter and Saturn can be interpreted as being the result of impact excitation by electrons of about 30 eV energies whereas that of Uranus can be fitted by invoking electrons with energies ~3 eV. The total power input required for the excitation of the electroglows (1.5×10^{12} W for Saturn and 1.7×10^{11} W for Uranus) might explain the elevated temperatures of the exospheres (~750 K for both Saturn and Uranus).

One new piece of information which might be essential to the understanding of the generation mechanisms of the electroglows concerns the fact that the altitude distributions of the ultraviolet emissions from limb-scanning measurements suggest that part of the excitations could be related to the collisional impact effect of energetic protons and/or fast hydrogen atoms impinging on the upper atmosphere of Saturn and Uranus[11,13].

Because of the ring absorption effect, energetic charged particles in the saturnian magnetosphere cannot diffuse inwards and reach the planetary atmosphere without undergoing nearly complete depletion[14]; the only effective way to inject energetic protons or fast hydrogen atoms then is via the process of charge-exchange recombination in the extended neutral gas cloud surrounding the planet[15,16]. In view of the extensive structure of the hydrogen corona at Uranus as revealed by the Voyager EUV observations[11], charge-exchange processes could be equally important in contributing to the electroglow emission. In the following, the physical model as well as a first-order estimate of the energy disposition rate to the upper atmosphere of Uranus will be described to evaluate the validity of this idea.

To begin with, note that the low-energy charged particle (LECP) experiment has determined that the magnetosphere of Uranus may be characterized as a low β plasma[4]. The maximum value of the ratio of the charged particle kinetic energy density (ε) to the magnetic field energy density ($B^2/8\pi$) as measured by Voyager 2 is $\beta \leq 0.1$ at $L \sim 15$. Taking this as a limit, we have as an extrapolation to the ring current particle flux in regions inside of the orbit of Miranda not scanned by the Voyager 2 spacecraft

$$\varepsilon(L) \sim \beta\, B_0^2/8\pi\, L^6 \qquad (1)$$

where $\beta < 0.1$ and B_0 (=0.23 gauss) is the equatorial surface field. With this expression, the total charged particle energy in a volume between L_a and L_b can be written as

$$E_{\text{total}} \sim \delta \int_{L_a}^{L_b} \varepsilon(L) \mathrm{d}V \sim \delta\, R_U^3 \int_{L_a}^{L_b} \varepsilon(L) \cdot 2\pi L^2\, \mathrm{d}L \qquad (2)$$

where δ is a form factor adjusting for the detailed distribution of the charged particles in the magnetic field. For $L_a \sim 2$ and $L_b \sim 5$, $E_{\text{total}} \sim 0.1\ \beta \times \delta \times B_0^2 \times R_U^3$ or $\beta \times \delta \times 10^{26}$ erg.

The limits of $L_a \sim 2$ and $L_b \sim 5$ are used in the above calculation as the charge-exchange process should be most efficient in this radial interval because of the large concentration of the neutral hydrogen atoms therein. Although the analytical expression of n_H as given in Broadfoot *et al.*[11] for L between 1.6 and 2 would predict a very small hydrogen density at 3-5 $R_U(n_H < 1\ \text{cm}^{-3})$, Shemansky and Smith[10] derived density curves (with $n_H \sim 10\text{-}100\ \text{cm}^{-3}$ for L between 2 and 4) corresponding to the hydrogen atoms ejected from the exobase in association with electroglow excitation. Using $n_H \sim 10\ \text{cm}^{-3}$ as a nominal value, the timescale for charge-exchange recombination is

$$t_{cx} \sim (n_H \sigma V)^{-1} \sim 10^6\ \text{s} \qquad (3)$$

where $\sigma V \sim 10^{-7}\ \text{cm}^3\ \text{s}^{-1}$ at particle energies ~15 keV (ref. 17). The energy dissipation rate of the ring current is thus (see ref. 17 for a review)

$$\dot{E}_{cx} \sim \frac{E_{\text{total}}}{t_{cx}} \sim \left(\frac{\beta}{0.1}\right) \times \left(\frac{\delta}{1}\right) \times \left(\frac{n_H}{10}\right) \times 10^{13}\ \text{W} \qquad (4)$$

Numerical calculations employing the Monte Carlo method similar to those by Prag *et al.*[18] and Prölss[19] have been performed for a centred dipole field and the results indicate that about 3-5% of the recombined energetic neutral particles will impact the planetary surface with concentration near the equator. The energy disposition rate to the dayside upper atmosphere is thus

$$\dot{E}_{cx}(\text{surface}) \sim \left(\frac{\beta}{0.1}\right) \times \left(\frac{\delta}{1}\right) \times \left(\frac{n_H}{10}\right) \times 5 \times 10^{11}\ \text{W} \qquad (5)$$

In the optimal condition with $\beta \sim 0.1$, $\delta \sim 1$, and $n_H \sim 10\ \text{cm}^{-3}$, $\dot{E}_{cx}(\text{surface}) \sim 5 \times 10^{10}$ W. In comparison, the energy inputs for the electroglow and nightside aurora are about 10^{11} W each at Uranus[11]. If the impact flux is assumed to be uniform over the disk, the energy flux contributed by the recombined fast neutrals should be of the order of $0.02\ \text{erg cm}^{-2}\ \text{s}^{-1}$ at maximum. This means that the fast neutrals from the charge exchange loss of the ring current system perhaps could be a significant source of excitation of the electroglow at Uranus which requires a total disposition rate of about $0.08\ \text{erg cm}^{-2}\ \text{s}^{-1}$.

Because straggling of the fast neutrals in the upper atmosphere would be followed by a succession of charge-exchange interaction, excitation (and hence atmospheric heating) and ionization of the neutral molecules via electron ejection[20], one consequence of charge-exchange processes in the magnetosphere would be an additional ionization of the H_2 atmosphere of Uranus. On the dayside hemisphere, this contribution may be easily masked by other effects; however, on the nightside hemisphere which is blocked from sunlight, the injection of fast neutrals could be partially responsible for the maintenance of a nightside ionosphere as revealed by the detection of Uranus electrostatic discharges (UED) by the planetary radio astronomy experiment[21]. The required energy disposition rate should be very much smaller than $0.02\ \text{erg cm}^{-2}\ \text{s}^{-1}$.

In the above discussion with emphasis on the possible relation between the fast neutral injection effect and the electroglows on Saturn and Uranus, limitations on observational data have rendered a number of uncertainties in the numerical estimates. For example, the adopted β value (~0.1) could have been too large and the assumed density distribution of the neutral hydrogen atoms in the extended corona may have been atypical. (Note that $\beta \sim 0.01$ and $t_{cx} \sim 10^5$ s would yield the same value of $\dot{E}_{cx}$ (surface).) On the other hand, some of the parameters used might be more appropriate for a disturbed interval of the magnetosphere rather than the quiet time situation. Furthermore, no account has been taken of the possibility that radial transport of the energetic charged particles could continue until reaching the upper atmosphere such that the efficiency of surface impact would be significantly enhanced. Also, the role of magnetospheric electrons is not discussed here, even though they could be important in maintaining a certain level of atmospheric ionization during the night-time[22]. There are therefore a number of open issues in need of detailed investigations. A very important factor as discussed here is the UVS observations of the signature of energetic protons–fast hydrogen impact excitations at Saturn and Uranus[11,15]. In a certain way, they could be regarded as remote sensing the charge-exchange process in the ring current systems. A determination of the corresponding energy disposition rates would clarify to what extent the energetics of the ring currents are coupled to the upper atmospheric dynamics of the outer planets.

Finally, note that additional energy sources other than charge-exchange loss of the ring current alone should be involved to account for the strong day-night asymmetry. Indeed, there is no obvious way that the charge-exchange process could be modulated so that it takes place predominantly only in the dayside hemisphere. The present estimate nevertheless suggests that this particular coupling effect between the magnetospheric plasma and the extended neutral exosphere could be quite significant in the excitation of atmospheric emission as well as heating and ionization of the nightside disk of Uranus.

Received 7 November 1986; accepted 20 January 1987.

1. Stone, E. C. & Miner, E. D. *Science* **233**, 39-43 (1986).
2. Ness, N. F. *et al. Science* **233**, 85-89 (1986).
3. Bridge, H. S. *et al. Science* **233**, 89-93 (1986).
4. Krimigis, S. M. *et al. Science* **233**, 97-102 (1986).
5. Vasyliunas, V. M. *Geophys. Res. Lett.* **13**, 621-623 (1986).
6. Selesnick, R. S. & Richardson, J. D. *Geophys. Res. Lett.* **13**, 624-627 (1986).
7. Brice, N. M. & Ioannidis, G. A. *Icarus* **13**, 173-183 (1970).
8. Brice, N. M. *J. geophys. Res.* **72**, 5193-5211 (1967).
9. Warwick, J. W. *et al. Science* **233**, 102-106 (1986).
10. Shemansky, D. E. & Smith, G. R. *Geophys. Res. Lett.* **13**, 2 (1986).
11. Broadfoot, A. L. *et al. Science* **233**, 74-79 (1986).
12. Clarke, J. T. *et al. J. geophys. Res.* (in the press).
13. Yelle, R. V., Sandel, B. R., Shemansky, D. E. & Kumar, S. *J. geophys. Res.* **91**, 8756-8770 (1986).
14. Fillius, W., Ip, W.-H. & McIlwain, C. E. *Science* **207**, 425-431 (1980).
15. Broadfoot, A. L. *et al. Science* **212**, 206-211 (1981).
16. Ip, W.-H. in *Planetary Rings* (ed. Brahic, A.) 575-596 (Cepadues-Editions, Toulouse, 1984).
17. Tinsley, B. A. *J. atmos. terr. Phys.* **42**, 227 (1981).

18. Prag, A. B., Morse, F. A. & McNeal, R. J. *J. geophys. Res.* **71**, 3141-3154 (1966).
19. Prölss, G. W. *Ann. Geophys.* **29**, 503-508 (1973).
20. Rees, M. H. *Planet. Space Sci.* **30**, 463-472 (1982).
21. Zarka, P. & Pedersen, B. M. *Nature* **323**, 605-608 (1986).
22. Lyons, L. R. & Richmond, A. D. *J. geophys. Res.* **83**, 2201-2204 (1978).

HCN and chromophore formation on Jupiter

James P. Ferris & Yoji Ishikawa

Department of Chemistry, Rensselaer Polytechnic Institute, Troy, New York 12180-3590, USA

The formation of HCN[1] and chromophores[2] are two of the major unsolved problems of the atmospheric chemistry of Jupiter. The question to be dealt with is the same in each case: how can these unsaturated organic compounds be formed in the highly reducing atmosphere[2] (89% H_2) present on Jupiter? The photolysis of ammonia/acetylene mixtures provides an answer to this question. Here we report the formation of both HCN and chromophores along with experimental data which support the premise that this photochemical process provides a route for the formation of both substances. It is not clear whether significant amounts of HCN are also formed by lightning on Jupiter[3,4].

It was first suggested by Kaye and Strobel[5] that HCN is formed on Jupiter by the photochemical addition of ammonia to acetylene. Reaction sequence (1)-(4) was outlined and compounds (a-d) were proposed as possible structures for C_2H_5N, the proposed HCN precursor formed in reaction (3). Neither HCN nor compounds (a-d) have been reported as products in previous investigations of the photolysis of ammonia/acetylene mixtures[6,7].

$$NH_3 \xrightarrow{h\nu} NH_2\cdot + H\cdot \quad (1)$$

$$H\cdot + C_2H_2 \rightarrow C_2H_3\cdot \quad (2)$$

$$C_2H_3\cdot + \cdot NH_2 \rightarrow C_2H_5N \quad (3)$$

$$C_2H_5N \xrightarrow{h\nu} HCN + CH_3\cdot + H\cdot \quad (4)$$

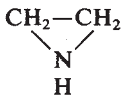

$CH_2{=}CHNH_2$ $CH_3CH{=}NH$ $CH_2{=}NCH_3$

(a) (b) (c) (d)

HCN is a product of the photolysis of ammonia in the presence of acetylene at room temperature (Table 1). Initial experiments (not described) established that HCN was formed from ammonia/acetylene mixtures where ammonia absorbed more than 98% of the light from a 185 nm source and more than 99.9% of the light from a 206.2 nm source (ref. 8). In addition, a brown, presumably oligomeric, deposit forms on the photolysis cell window.

Table 1 Variations in the yield of HCN, brown oligomers and HCN precursors

Temperature (K)	H_2 (torr)	HCN* ($m \times 10^5$)	Brown oligomers†	HCN precursors‡
298	0	10.1 (0.9)	0.24 (0.005)	0
298	77.5	6.4 (2.7)	0.09 (0.04)	0
178	0	2.9 (0.75)	0.14 (0.01)	0.12 (0.03)
178	77.5	0.55 (0.13)	0.09 (0.04)	0.09 (0.12)
178	700	0.39 (0.14)	0.05 (0.01)	0.27 (0.10)

In these experiments NH_3 at 5 torr and 2.5 torr acetylene were irradiated for 8 h; standard deviations given in parentheses.
* Monitored by the method of Kruse and Mellon[9,10].
† Monitored by absorbance at 300 nm.
‡ Monitored by absorbance at 220 nm.

Photolyses were performed in the presence of hydrogen and at lower temperatures to determine if the same products were formed using conditions close to those prevalent in the atmosphere of Jupiter (Table 1). The HCN yield decreased by 70% when the temperature was lowered to 178K and there was a further 80% decrease in the yield when 77.5 torr of hydrogen was added to the photolysis mixture. No further decrease was observed when 700 torr of hydrogen was used instead of 77.5 torr (Table 1).

A HCN precursor fraction was detected by an enhanced ultraviolet absorption at 220 nm when the photolyses were performed at 178K and the photolysis cell was warmed to room temperature for UV analysis (Table 1). These compounds condense on the cell wall at 178K where they are no longer subject to ultaviolet irradiation. Combination gas chromatographic-mass spectral analysis established that acetonitrile (e) and acetaldehyde ethylidenehydrazone (f) were the major nitrogen-containing products in the precursor fraction. Compounds (a-d) were not detected in this fraction.

A reaction pathway to HCN can be proposed on the basis of this and other research described below[11,12]. The reaction process is initiated by the photodissociation of ammonia (1) since it was established that it is absorbing more than 98% of the light. The addition of a hydrogen atom to acetylene (2) is the next step since the pseudo first order rate constant for hydrogen atom addition[11] is 3,000 times greater than $NH_2\cdot$ addition at 178K[12]. Steps (5)-(9) provide a concise and plausible speculative rationale for the formation of the observed HCN precursors (e) and (f).

$$NH_2\cdot + CH_2{=}CH\cdot \rightarrow CH_2{=}CHNH_2 \quad (5)$$

$$H\cdot + CH_2{=}CHNH_2 \rightarrow CH_2{=}CHNH\cdot + H_2 \quad (6)$$

$$CH_2{=}CHNH\cdot \rightarrow CH_3CH{=}N\cdot \quad (7)$$

$$CH_3CH{=}N\cdot \rightarrow CH_3C{\equiv}N\ (e) + H\cdot \quad (8)$$

$$2\,CH_3CH{=}N\cdot \rightarrow CH_3CH{=}NN{=}CHCH_3\ (f) \quad (9)$$

$$CH_3CH{=}NN{=}CHCH_3 \xrightarrow{h\nu} CH_3C{\equiv}N + CH_3CH{=}NH \quad (10)$$

$$CH_3C{\equiv}N + H\cdot \rightarrow [CH_3CH{=}N]\cdot \rightarrow HCN + CH_3\cdot \quad (11)$$

The photolysis of both precursors ultimately results in the formation of HCN. Irradiation of (f) results in the formation of acetonitrile (e) with a quantum yield of 0.5 (10) (see ref. 13). The hydrogen-atom-initiated conversion of acetonitrile to HCN (11) proceeds with high efficiency and does not require light absorption by the acetonitrile[14]. We observed that HCN is formed by the photolysis of 5 torr ammonia in the presence of 0.3 torr of acetonitrile using a 185 nm light source.

The vapour pressure of acetonitrile was estimated to ascertain that its photolysis to HCN is a plausible reaction in the Jovian atmosphere. Since there are no reports of the vapour pressure of acetonitrile in the 150-200K range, its vapour pressure was estimated by comparison with that of the vapour pressure of HCN. The vapour pressure of HCN was calculated[15] to be 4×10^{-4} torr at 150K which is equivalent to a mixing ratio of 5×10^{-7} at 1 bar. This vapour pressure is 250 times greater than the measured mixing ratio on Jupiter[1] of 2×10^{-9}. Since the vapour pressure of acetonitrile is one-tenth that of HCN in the 220-273K range[16], it can be estimated that the vapour pressure of acetonitrile at 150K is one-tenth that of HCN or 25 times greater than the observed HCN mixing ratio. It can be concluded that acetonitrile is sufficiently volatile at 150K for the photochemical generation of the levels of HCN observed in the atmosphere of Jupiter.

The yield of chromophoric oligomers decreases by about 60% when 77.5 torr of hydrogen is added to the photolysis mixture (Table 1). Little or no additional decrease in oligomer formation is observed on addition of 700 torr hydrogen or lowering the temperature to 178K. These findings suggest that the hydrogen-